1521-009X/46/5/525–531$35.00
DRUG METABOLISM AND DISPOSITION

https://doi.org/10.1124/dmd.117.078444
Drug Metab Dispos 46:525–531, May 2018

Generation and Characterization of a CYP2C11-Null Rat Model by Using the CRISPR/Cas9 Method[S]

Yuan Wei, Li Yang, Xiaoyan Zhang, Danjuan Sui, Changsuo Wang, Kai Wang, Mangting Shan, Dayong Guo, and Hongyu Wang

School of Pharmacy, Jiangsu University, Zhenjiang, Jiangsu, China (Y.W., L.Y., X.Z., D.S., C.W., K.W.); MtC BioPharma Co. Ltd., Nanjing, Jiangsu, China (M.S.); and Model Animal Research Center, Nanjing Biomedical Research Institute, Nanjing University, Nanjing, Jiangsu, China (D.G., H.W.)

Received September 10, 2017; accepted February 8, 2018

ABSTRACT

CYP2C11 is involved in the metabolism of many drugs in rats. To assess the roles of CYP2C11 in physiology and drug metabolism, a *CYP2C11*-null rat model was generated using the clustered regularly interspaced short palindromic repeats (CRISPR)/Cas9 method. A 2-base pair insertion was added to exon 6 of *CYP2C11* in Sprague-Dawley rats. CYP2C11 was not detected by western blotting in liver microsomes of *CYP2C11*-null rats. No off-target effects were found at 11 predicted sites of the knockout model. The *CYP2C11*-null rats were viable and had no obvious abnormalities, with the exception of reduced fertility. Puberty in *CYP2C11*-null rats appeared to be delayed by ~20 days, and the average litter size fell by 43%. Tolbutamide was used as a probe in this drug metabolism study. In the liver microsomes of *CYP2C11*-null rats, the V_{max} and intrinsic clearance values decreased by 22% and 47%, respectively, compared with those of wild-type rats. The K_m values increased by 47% compared with that of wild types. However, our pharmacokinetics study showed no major differences in any parameters between the two strains, in both males and females. In conclusion, a *CYP2C11*-null rat model was successfully generated and is a valuable tool to study the in vivo function of CYP2C11.

Introduction

CYP2C11 is the most abundant cytochrome P450 (P450) in the livers of adult male rats, where it accounts for ~50% of the total P450s (Morgan et al., 1985; Banerjee et al., 2015). CYP2C11 is exclusively expressed in the livers of adult male rats; this male-specific expression is activated by the male pattern of plasma growth hormone pulsation (Choi and Waxman, 2000). CYP2C11 is involved in the metabolism of a large number of drugs, including phenytoin, ibuprofen, tolbutamide (TOL), and S-warfarin (Nedelcheva and Gut, 1994; Rendic and Di Carlo, 1997; Wójcikowski et al., 2013). It also plays a role in many endogenous biochemical reactions, such as the hydroxylation of endogenous steroids, the epoxygenation of arachidonic acid, and the hydroxylation of vitamin D (Roman, 2002; Barbosa-Sicard et al., 2005; Rahmaniyan et al., 2005; Wójcikowski et al., 2013). The function and regulation of CYP2C11 has been extensively studied in previous reports; however, the in vivo roles of CYP2C11 in physiologic processes and drug metabolism are still not very clear.

Since the mid-1990s, genetic knockout mouse models have been used to study the in vivo function of P450s (Mckinnon and Nebert, 1998; Gonzalez and Kimura, 2003). Those models have been important tools for the study of clinically relevant P450 drug metabolism (Muruganandan and Sinal, 2008). However, these mouse models have two major disadvantages. First, the plasma and tissue volume of the mouse are relatively small; therefore, more advanced analytic instruments and methods are required. Second, the intra-species differences between mice and humans are large (Gonzalez and Yu, 2006), especially in pharmacokinetic and toxicological studies. Based on these factors, P450 genetic knockout rat models would be a better choice since rats are larger in size and their physiologic characteristics are closer to those of humans (Wang et al., 2016). Unfortunately, due to the instability of rat embryonic stem cell lines, the generation of genetic knockouts in the rat is much more difficult than in the mouse.

Clustered regularly interspaced short palindromic repeats (CRISPR)/Cas9 technology was introduced to eukaryotic cells in 2013 and showed efficient genome editing effects (Cong et al., 2013). The first knockout rat model was successfully generated using CRISPR/Cas9 technology in 2014. Three rat DNA methyltransferase genes (Dnmt1, Dnmt3a, and Dnmt3b) were targeted and LoxP sites were inserted into the genes using a circular donor vector as a template (Ma et al., 2014). The first report of a P450-knockout rat model was published in 2016, where knockout of the *CYP2E1* gene arrested the metabolic function of CYP2E1 and delayed the clearance of chlorzoxazone (Wang et al., 2016).

The aims of our study were to generate a *CYP2C11*-knockout (*CYP2C11*-null) rat model using CRISPR/Cas9 technology, and to characterize the general phenotypes of this model and compare them to those of wild-type (WT) Sprague-Dawley rats. Furthermore, TOL was used as a probe drug to study in vitro and in vivo metabolism in this rat model.

This work was funded by grants from the National Natural Science Foundation of China [Grants 81102522, 81373480, and 81573529], and the Natural Science Foundation of Jiangsu Province [Grant BK2011473].
https://doi.org/10.1124/dmd.117.078444.
[S]This article has supplemental material available at dmd.aspetjournals.org.

ABBREVIATIONS: bp, base pair; CRISPR, clustered regularly interspaced short palindromic repeats; DHEA, dehydroepiandrosterone; PPAR, peroxisome proliferator-activated receptor; P450, cytochrome P450; sgRNA, single guide RNA; TOL, tolbutamide; WT, wild type.

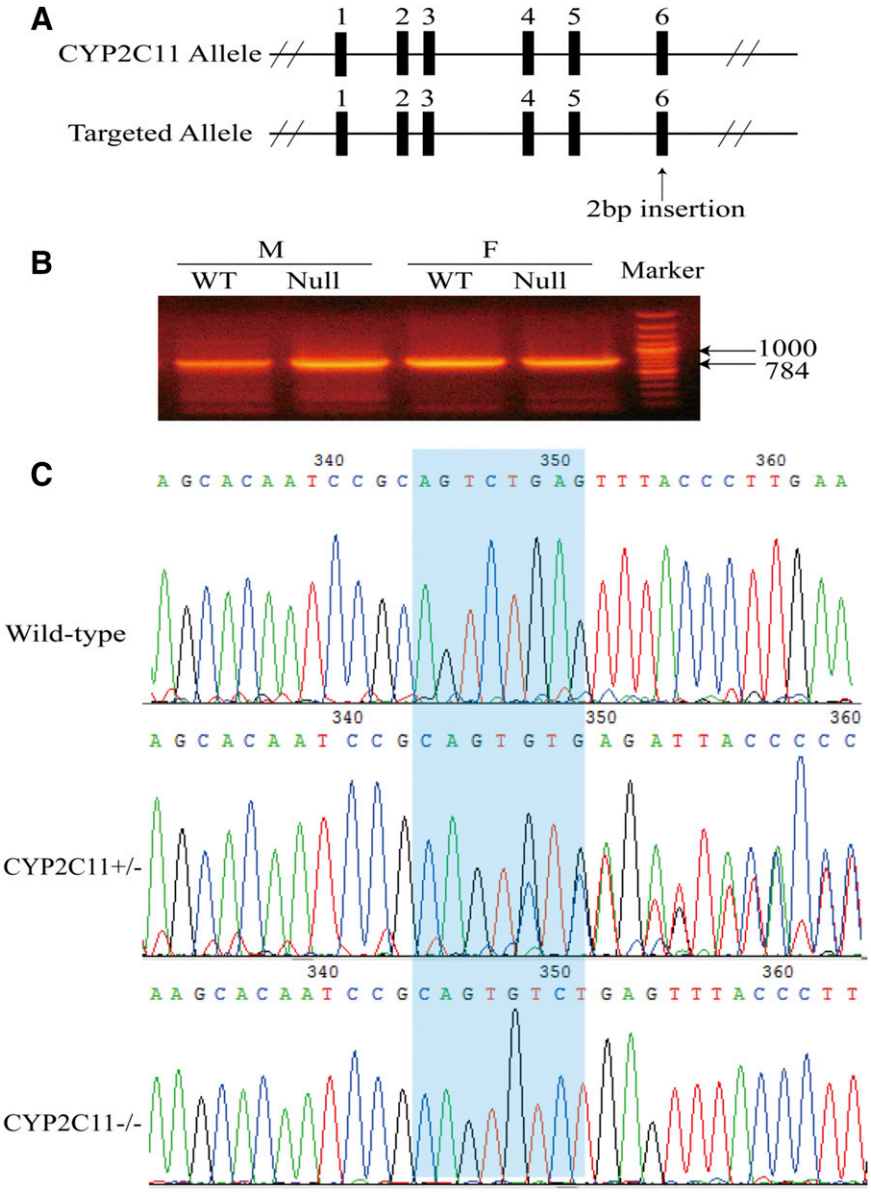

Fig. 1. Confirmation of gene targeting in *CYP2C11*-null rats. (A) Schematic of the exonic structure of the *CYP2C11* gene in rats. Exons are shown as black boxes. The 2-bp insertion was added to exon 6. (B) DNA fragments (approximately 784 bp) amplified from CYP2C11$^{-/-}$ and WT rats. (C) Genotyping results for *CYP2C11*$^{-/-}$, *CYP2C11*$^{+/-}$, and WT rats; 2 bp (GT) were inserted in exon 6 of *CYP2C11* in the knockout alleles.

Materials and Methods

Chemicals and Reagents. Tolbutamide (>99% purity) was purchased from Sigma-Aldrich (St. Louis, MO). Chlorpropamide (>99% purity) was purchased from J&K Scientific Co. Ltd. (Beijing, China). 4-hydroxy tolbutamide (>98% purity) was purchased from Cayman Chemicals Co. (Ann Arbor, MI). NADPH (>98% purity) was purchased from Aladdin Industrial Co. (Shanghai, China). Acetonitrile and methanol, as well as all other reagents, were purchased from Sinopharm Chemical Reagent Co. Ltd. (Shanghai, China).

Generation of CYP2C11-Null Rats. Two pairs of single guide RNA (sgRNA) primers were designed: sgRNA1 (forward primer: 5′-GCTACTG-TAACTGACATGTT-3′; reverse primer: 5′-AACATGTCAGTTACAGTAGC-3′) and sgRNA2 (forward primer: 5′-TCAAGGGTAAACTCAGACTG-3′; reverse primer: 5′-CAGTCTGAGTTTACCCTTGA-3′). The sgRNAs were produced using the T7 Transcription Kit (Thermo Fisher Scientific Inc., Waltham, MA), recovered using phenol/chloroform extraction and ethanol precipitation, and finally dissolved in nuclease-free water. For *Cas9* mRNA construction, a *Cas9* expression vector was linearized with AgeI (New England Bioscience, Ipswich, MA); the expressed *Cas9* mRNA was purified with the RNeasy Mini Kit (Qiagen, Valencia, CA). Purified sgRNA1 (100 ng/μl) or sgRNA2 (100 ng/μl), and *Cas9* mRNA (50 ng/μl) were co-injected into zebrafish zygotes to determine their activities.

The sgRNA2 primer set was injected into Sprague-Dawley rat monocytic embryos with the *Cas9* mRNA since sgRNA2 had higher activity in the zebrafish. The F_0 pups were screened by genomic DNA sequencing to identify heterozygous *CYP2C11*$^{+/-}$ founders. The confirmed founders were transferred from the Model Animal Research Center of Nanjing University to the Laboratory Animal Center of Jiangsu University for breeding. The animal facilities at Nanjing University and Jiangsu University are both accredited by the Association for Assessment and Accreditation of Laboratory Animal Care (https://www.aaalac.org/). All animal breeding and experimental procedures were carried out in accordance with the Guide for the Care and Use of Laboratory Animals (http://sbcold.ujs.edu.cn/dongwu) and were approved by the Institutional Animal Care and Use Committees at Nanjing University and Jiangsu University.

Off-Target Analysis. Potential off-target sites in the rat genome were identified using TagScan (http://ccg.vital-it.ch/tagger) based on the sgRNA2 sequence (TCAAGGGTAAACTCAGACTG). Detailed sequences around the potential off-target sites were obtained from the University of California Santa Cruz database (http://genome.ucsc.edu/). Polymerase chain reaction was performed for each sequence using the corresponding primers (Supplemental Table 1) with genomic DNA templates from *CYP2C11*-null rats. The polymerase chain reaction products were then sequenced by Sangon Biotech Co. (Shanghai, China) and compared with their corresponding sequences in the University of California Santa Cruz database.

TABLE 1

Viscera indices in CYP2C11-null and WT rats at 60 days old

All values are shown as the mean ± S.D., n = 6. *P < 0.05 compared with that of WT rats.

Viscera Indices[a]	Male		Female	
	WT	Null	WT	Null
Body weight (g)	254 ± 7.46	234.18 + 27.70	148.32 ± 4.17	162.97 + 21.68
Liver (%)	6.47 ± 0.60	5.92 ± 2.07	5.16 ± 0.29	5.98 ± 2.72
Spleen (%)	0.40 ± 0.05	0.29 ± 0.03	0.25 ± 0.03	0.25 ± 0.03
Lungs (%)	0.74 ± 0.11	0.68 ± 0.08	0.79 ± 0.07	0.64 ± 0.15
Kidney (%)	1.24 ± 0.14	1.08 ± 0.17	0.97 ± 0.05	0.95 ± 0.17
Testis (%)	1.00 ± 0.19	1.25 ± 0.12		
Brain (%)	0.89 ± 0.04	0.61 ± 0.07*	0.87 ± 0.05	0.76 ± 0.13

[a]Viscera index = tissue weight (g)/rat body weight (g) × 100%.

Characterization of CYP2C11-Null Rats. To identify any abnormalities in the *CYP2C11*-null rats, 2-month-old rats were sacrificed with CO_2 and dissected for further study. The viscera indices (defined as the ratio of tissue weight to body weight) were calculated and compared between the *CYP2C11*-null and WT Sprague-Dawley rats. Tissue samples (including liver, spleen, kidney, small intestine, and testis) were fixed in phosphate-buffered saline with 10% paraformaldehyde; thereafter, the samples were embedded in paraffin. Tissue sections (5 μm) were cut and stained with hematoxylin and eosin. Histopathological analysis was then performed.

Rat liver microsomes were prepared from liver tissues by differential centrifugation, as described previously (Ding and Coon, 1990). The protein contents of the microsomal suspensions were determined using a bicinchoninic acid kit (Beyotime, Nantong, China). Western blotting was performed to study the protein expression levels of the major P450s. Each lane was loaded with 5-μg liver microsomal protein from an individual rat (Gu et al., 2003). Glyceraldehyde-3-phosphate dehydrogenase and β-actin were not used as reference proteins since they were barely present in liver microsomes. Instead, Ponceau S staining was used to confirm that the same amount of protein was loaded into each lane.

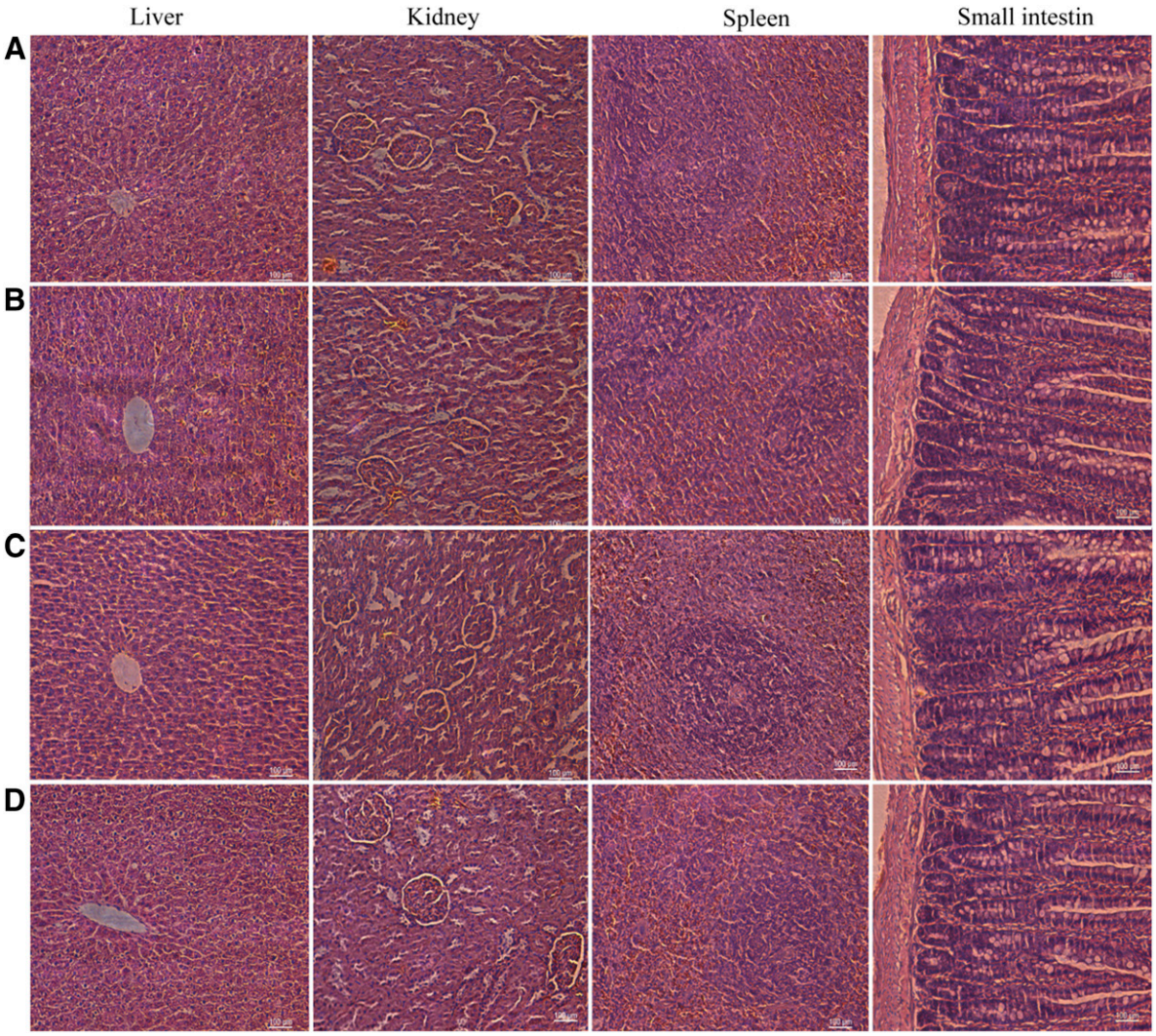

Fig. 2. Micrographs of rat liver, kidney, spleen, and small intestine sections with hematoxylin and eosin staining (original magnification, 100×): (A) male WT rats; (B) male *CYP2C11*-null rats; (C) female WT rats; (D) female *CYP2C11*-null rats.

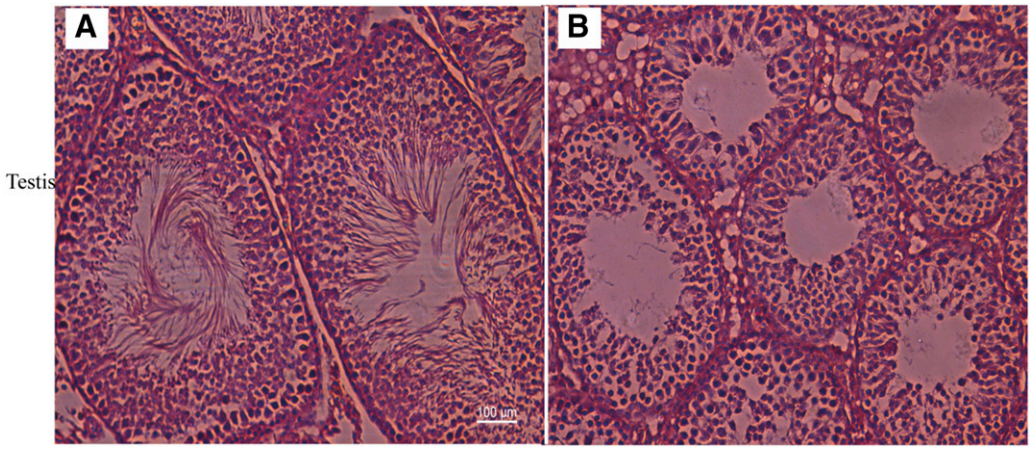

Fig. 3. Micrographs of rat testis sections with hematoxylin and eosin staining (original magnification, 100×): (A) male WT rats; (B) male *CYP2C11*-null rats.

The membranes were then probed with antibodies against CYP2C11 (PA3-034, rabbit polyclonal; Thermo Fisher Scientific, Waltham, MA), CYP1A2 (sc-53241, mouse monoclonal IgG_1), CYP2B (sc-73546, mouse monoclonal IgG_1; Santa Cruz Biotechnology, Santa Cruz, CA), CYP2D (PAB19502, rabbit polyclonal; Abnova, Teipeh, Taiwan, China), CYP2E1 (BML-CR3271-0100, rabbit polyclonal; Enzo, Farmingdale, NY), CYP3A (sc-25845, rabbit polyclonal IgG), CYP4A1 (sc-53248, mouse monoclonal IgG_{2b}), and cytochrome P450 reductase (sc-55477, mouse monoclonal IgG_{2a}; Santa Cruz Biotechnology) overnight at 4°C, and then incubated with the corresponding horseradish peroxidase–coupled secondary antibody. The blots were visualized using enhanced chemiluminescence solution (Millipore, Billerica, MA). Chemiluminescent signals were detected and analyzed using a ChemiDoc XRS imaging system (BioRad, Hercules, CA).

Fertility Test for CYP2C11-Null Rats. For the breeding test, 60-day-old male and female rats were paired for the breeding test. One breeding pair consisted of one female and one male. Vaginal smears were performed every morning to confirm the presence of spermatozoa, which indicated copulation. The ages of the female rats on the first day of pregnancy and litter sizes on the day of delivery were recorded.

TOL Metabolism in CYP2C11-Null Rats. The liver microsomes of WT and *CYP2C11*-null rats were obtained and their protein contents were determined. The incubation mixtures consisted of 1 mg/ml liver microsomes and varied concentrations (100, 200, 500, 1000, or 2000 μM) of TOL. The reactions were preincubated for 5 minutes at 37°C, and then 5 mM $MgCl_2$ and 1 mM β-NADPH were added to start the reaction (250 μl final volume). The reaction was performed for 30 minutes in a 37°C water bath. The reaction was then terminated by 100 μl ice-cold methanol solution (containing 7 μM chlorpropamide). The reaction mixtures were extracted with 400 μl ice-cold ethylacetate, vigorously vortexed for 1 minute, and then centrifuged at 9600*g* at 4°C for 10 minutes. The organic phase was transferred to a clean tube, and the extraction process was repeated for a second time. The supernatant was dried under nitrogen stream, and the residue was reconstituted in 100 μl methanol for high-performance liquid chromatography analysis.

For the pharmacokinetics study, each group contained six rats. Rats were fasted overnight, but allowed free access to water before dosing. TOL, in 0.5% carboxymethyl cellulose/sodium solution, was administered orally to WT and *CYP2C11*-null rats by gavage at a dose of 10 mg/kg. Blood samples (approximately 200 μl) were collected from the orbital venous plexus at 0.5, 1, 1.5, 2, 3, 4, 6, 9, 12, 24, and 36 hours. Blood samples were centrifuged at 4000*g* for 15 minutes and the supernatant plasma was transferred to a new tube. Thereafter, 200 μl ice-cold ethylacetate containing internal standard and 5 μl 1 N HCl were added to 50 μl plasma, vigorously vortexed for 2 minutes, and then centrifuged at 8000*g* at 4°C for 10 minutes. The supernatant was transferred to a clean tube, and the process was repeated to extract all remaining plasma. The supernatant was dried under nitrogen stream, and the residue was reconstituted in 100 μl methanol for high-performance liquid chromatography analysis.

High-performance liquid chromatography analysis was performed using the Shimadzu LC-20A with a UV detector (Shimadzu Corporation, Kyoto, Japan). The injection volume was 20 μl. An Agilent C18 column (5 μm, 4.6 × 250 mm; Agilent Technologies, Santa Clara, CA) was used and the column temperature was 40°C. The mobile phase consisted of 45% methanol, 15% acetonitrile, and 40% phosphate buffer; the flow rate was 1 ml/min. The detection wavelength was set at 226 nm. Peak areas of hydroxytolbutamide and chlorpropamide were recorded.

Statistical Analysis. Data are presented as the mean ± S.D. The data were evaluated for statistical significance by one-way analysis of variance. SPSS 13.0 (IBM, New York, NY) was used for analysis. A value of $P < 0.05$ was considered statistically significant.

Results

Generation of CYP2C11-Null Rats. Three founders with different mutations [6- and 7-base pair (bp) deletion, and 2-bp insertion] in exon 6 of *CYP2C11* were obtained from the Model Animal Research Center of Nanjing University. The founder with the 6-bp deletion was discarded since the open reading frame of *CYP2C11* was not shifted. The founder with the 7-bp deletion was infertile. Therefore, only the founder with the 2-bp insertion was used for further studies. Genotyping results for $CYP2C11^{-/-}$, $CYP2C11^{+/-}$, and WT rats are shown in Fig. 1. DNA fragments of approximately 784 bp were amplified from rat genomic DNA and used for sequencing (Fig. 1B). Two base pairs (GT) were inserted into exon 6 of *CYP2C11* in the knockout alleles (Fig. 1C).

Off-Target Analysis. For sgRNA2, 11 potential off-target sites were found with TagScan (Supplemental Fig. 1). The sequencing results showed no difference between the amplified sequences from *CYP2C11*-null rats and their corresponding sequences in the University of California Santa Cruz database. No off-target effects were detected for the 11 potential sites in our knockout model.

General Characterization of CYP2C11-Null Rats. Homozygous *CYP2C11*-null rats were fertile and appeared normal in their general appearance and social interactions. The viscera indices of *CYP2C11*-null and WT rats are shown in Table 1. The viscera indices of *CYP2C11*-null rats showed no substantial differences compared with those of WT rats, except for the brain index, which showed a considerable decrease in the *CYP2C11*-null rats (Table 1).

The histopathological results are shown in Fig. 2. For tissue sections of the liver, spleen, kidney, and small intestine, no obvious morphologic changes were observed between the *CYP2C11*-null and WT rats. In the testes of *CYP2C11*-null rats, fewer mature spermatozoa were observed than in WT rats. Furthermore, fewer primary

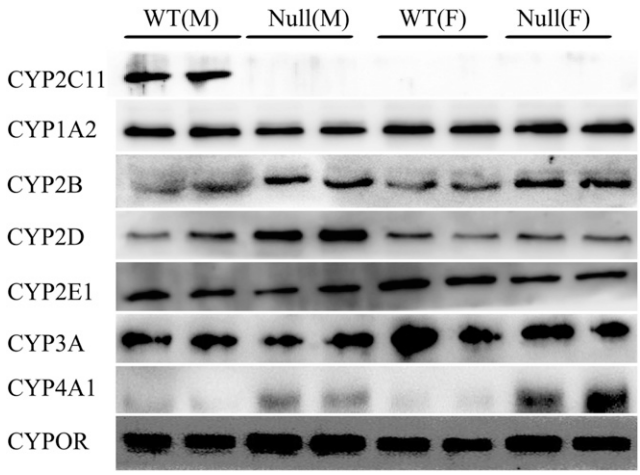

Fig. 4. Western blot analysis of several P450 isoforms (CYP2C11, CYP1A2, CYP2B, CYP2D, CYP2E1, and CYP4A1) and P450 reductase (CYPOR) in the livers of *CYP2C11*-null and WT rats. CYP2C11 was not detected in the liver microsomes of *CYP2C11*-null rats. CYP2B, CYP2D, and CYP4A1 expressions were increased in *CYP2C11*-null males, while CYP2B and CYP4A1 expressions were increased in *CYP2C11*-null females.

and secondary spermatocytes were found in the seminiferous tubules of *CYP2C11*-null rats (Fig. 3).

Western Blot Analysis. As shown in Fig. 4, CYP2C11 protein was not detected in the liver microsomes of *CYP2C11*-null rats. The concentrations of CYP2B, CYP2D, and CYP4A1 showed substantial increases in male *CYP2C11*-null rats, while increases in CYP2B and CYP4A1 were also observed in female knockout rats. No changes were found in the expression of any other tested P450s or cytochrome P450 reductase in *CYP2C11*-null rats.

Fertility of the CYP2C11-Null Rats. The average age of WT rats at copulation plug detection day was 69 ± 5 days. The average age of *CYP2C11*-null rats at copulation plug detection day was 89 ± 10 days ($P < 0.05$). The puberty of *CYP2C11*-null rats appeared to be delayed by ~20 days and the average litter size fell by 43% (Table 2).

TOL Metabolism in CYP2C11-Null Rats. TOL was selected as a substrate to compare CYP2C11 enzyme activity in the WT and *CYP2C11*-null rats. The formation rate of hydroxytolbutamide was used to calculate enzyme kinetic parameters. The V_{max}, K_m, and intrinsic clearance (V_{max}/K_m) are shown in Table 3. The V_{max} and intrinsic clearance values of the knockout rats decreased by 22% and 47%, respectively, compared with those of the WT rats. The K_m value of the knockout rats increased by 47% compared with that of the WT rats (Table 3). In other words, the hepatic microsome of the *CYP2C11*-null rats had a lower affinity to TOL and a lower reaction velocity; this was probably caused by the absence of CYP2C11.

The blood concentration of TOL in each group reached a maximum at 1–6 hours (Fig. 5). The calculated pharmacokinetic parameters are summarized in Table 4. There were no considerable differences in any parameters between the two strains in both males and females. However, within the same strain, TOL showed a faster clearance in males than in females. These results indicated that the clearance patterns of TOL were almost the same in *CYP2C11*-null and WT rats in vivo.

TABLE 2

Fertility of WT rats and CYP2C11-null rats

All values are shown as the mean ± S.D., n = *20.* *P < *0.05 compared with that of WT rats.*

Group	Age at Copulation Plug Detection	Number of Fertile Pairs	Litter Size
	Day		
WT	69 ± 5	20	11 ± 3
Null	89 ± 10*	18	6 ± 2*

TABLE 3

Kinetics of TOL metabolism with CYP2C11-null or WT rat liver microsomes

All values are shown as the mean ± S.D., n = *3.* **P < *0.001 compared with that of WT rats.*

	K_m	V_{max}	CL_{int}
	μM	*pmol/min/mg protein*	*μL/mg/min*
Null	893.37 ± 25.15**	1082.40 ± 30.48**	1211.59**
WT	605.76 ± 13.84	1384.68 ± 31.63	2285.86

CL_{int}, intrinsic clearance.

Discussion

In rats, the CYP2C subfamily consists of members including CYP2C6, CYP2C7, CYP2C11, CYP2C12, CYP2C13, CYP2C22, CYP2C23, CYP2C24, CYP2C79, CYP2C80, and CYP2C81 (Heil et al., 2005; Martignoni et al., 2006). The homology between members of the CYP2C subfamily may present difficulties in generating the *CYP2C11*-null rat model. When designing the targeting strategy, we avoided exons with high homology, and found that exon 6 of the *CYP2C11* gene was a good target. The sequencing results of the *CYP2C11*-null rat model confirmed that our targeting strategy was successful; our experience could be used to improve similar gene targeting studies.

We analyzed the coding sequence of the targeted-*CYP2C11* gene and found that the GT insertion created a premature stop codon, and truncated the protein length to 291 amino acids. At least two amino acid residues (V362 and F476), critical for substrate binding of CYP2C11 (Wang et al., 2009), were lost in the truncated protein. These facts suggested that targeted CYP2C11 had no functions.

Recent studies have shown that CRISPR/Cas9 systems may lead to mutations in potential off-target sites with similar sequences to the guiding RNA (Lin et al., 2014). Several online databases have been reported to be useful in identifying potential off-target sites, such as E-CRISP (Heigwer et al., 2014), Cas-OFFinder (Bae et al., 2014), and COSMID (Cradick et al., 2014). We used TagScan (Lin et al., 2014) to predict potential off-target sites, and confirmed the absence of mutations at the predicted sites through detailed sequencing. However, a recent study showed that DNA mutations could happen at nonpredicted sites in CRISPR/Cas9-mediated gene editing (Schaefer et al., 2017). Thus, whether random mutations occurred in our *CYP2C11*-null rat model needs to be further verified.

CYP2C11 is a male-specific androgen 2α- and 16α-hydroxylase found in the adult rat liver, and participates in the hydroxylation of testosterone and androstenedione (Waxman, 1988; Ryan and Levin, 1990; Wójcikowski et al., 2013). It was possible that the knockout of *CYP2C11* could affect testosterone metabolism in male rats. In our study, we found that the number of spermatozoa was reduced in the testes of the knockout rats, and that puberty appeared to be delayed by ~20 days. The average litter size of knockout breeding pairs also fell by 43%. We tried to determine the plasma testosterone levels in adult male rats for both *CYP2C11*-null and WT strains. However, individual differences in both stains were too large to draw any conclusions (data not shown).

In our study, the brain-to-body weight ratio of male knockout rats was decreased by 31% compared with WT rats (from 0.89 to 0.61). Interestingly, the brain-to-body weight ratio (%) in different rat strains ranged from about 0.517 to 1.798 (Japan National Bio Resource Project, http://www.anim.med.kyoto-u.ac.jp/NBR/strainsx/OW_list.aspx).

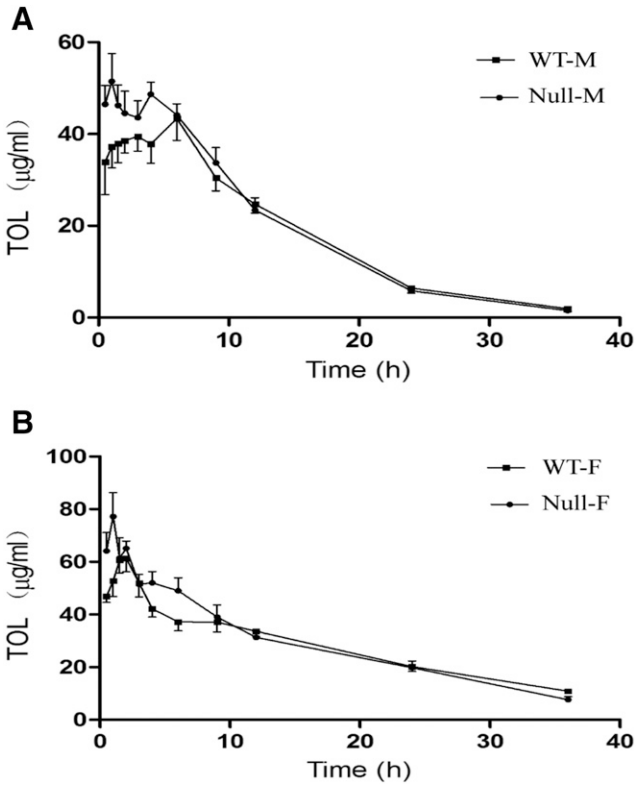

Fig. 5. Mean plasma concentration-time curves of TOL after intragastrical administration at a dose of 10 mg/kg in WT Sprague-Dawley and *CYP2C11*-null rats: (A) male rats; (B) female rats. All values are shown as the mean ± S.D., $n = 6$.

This fact suggested that the 31% drop in brain-to-body weight ratio in the *CYP2C11*-null rats is not necessarily a major concern. However, the role of *CYP2C11* gene knockout in rat brain weight loss requires further study.

The upregulation of CYP2B and CYP4A1 protein was detected in the livers of both males and females of *CYP2C11*-null rats. The constitutive expression and the induction of hepatic *CYP2B* were associated with nuclear receptors including the constitutive androstane, pregnane X, and retinoid X receptors (Honkakoski and Negishi, 2000). Induction of the rat hepatic *CYP2B* genes by phenobarbital was thought to occur by binding of the constitutive androstane receptor/retinoid X receptor heterodimer to a distal promoter of the *CYP2B* genes known as the phenobarbital-responsive enhancer module (Honkakoski and Negishi, 2000). The induction of CYP4A enzymes was mediated by peroxisome proliferator-activated receptors (PPARs). PPARs bound to peroxisome proliferator response elements of the *CYP4A1* gene as heterodimers with retinoid X receptors (Johnson et al., 1996). Dehydroepiandrosterone (DHEA), an androstane, had been found to be an endogenous agonist of the constitutive androstane receptor and induces the liver expression of CYP2B (Kőhalmy et al., 2007; Timsit and Negishi, 2014). Interestingly, DHEA and its oxidative metabolites had been reported to activate PPARα, and consequently to induce *CYP4A* in rat hepatocytes (Wu et al., 1989; Webb et al., 2006). Also, negative regulation of *CYP2C11* expression by DHEA treatment had also been demonstrated in rats, although PPARα coexpression did not seem to be required for this negative regulation (Ripp et al., 2003). Based on these facts, it could be speculated that CYP2C11 was important in the homeostasis of DHEA, and knockout of *CYP2C11* might cause buildup of DHEA and alter the expression of other P450 enzymes. Nonetheless, it remains a puzzle why the expression of CYP2B and CYP4A was upregulated in female rats, where CYP2C11 is not detected in the adult liver. It may be warranted to examine CYP2C11 expression in liver and other tissues of female rats during early development, when it might have an imprinting effect on the expression of CYP2B and CYP4A.

The upregulation of CYP2D was only detected in males of knockout rats. Rat liver CYP2D had been considered as resistant to direct hormonal regulation (Wójcikowski and Daniel, 2009). However, it was reported that repeated restraint stress and epinephrine treatment could induce the hepatic expression of CYP2D1/2 in male rats (Daskalopoulos et al., 2012). The role of stress in the induction of hepatic CYP2D of *CYP2C11*-null males needs to be further addressed.

TOL was used as a probe to evaluate CYP2C11 activity in several studies (Matsunaga et al., 2001; Wang et al., 2010). In our in vitro study, we found considerable differences in TOL metabolism when incubated with hepatic microsomes from *CYP2C11*-null and WT rats. However, no major differences were found in the in vivo pharmacokinetic analysis of TOL between the WT and *CYP2C11*-null rats. Since substantial differences were observed in the pharmacokinetics between male and female rats, which is consistent with previous reports (Tan et al., 2011), the results of our pharmacokinetic analysis of TOL appear to be reliable. The apparent contradictory results between our in vitro and in vivo experiments may be due to the following reasons. First, the knockout of *CYP2C11* could have been compensated by the enhanced expression of other P450s, and TOL may have interacted with those P450s more readily in the in vivo experiment. Furthermore, TOL was not a CYP2C11-specific substrate (Veronese et al., 1990; Cribb et al., 1995; Brown et al., 2007; Dostalek et al., 2007; Velenosi et al., 2012); other members of the CYP2C subfamily could contribute to the in vivo metabolism of TOL. Therefore, more specific reactions, such as testosterone 2α- and 16α-hydroxylation, and warfarin 4′- and 6-hydroxylation, will be analyzed in this *CYP2C11*-null rat model.

Epoxyeicosatrienoic acids can effectively regulate blood pressure, and CYP2Cs are major epoxyeicosatrienoic acid epoxygenases in rat kidneys (Holla et al., 1999; Capdevila et al., 2007; Imig, 2010). It was reported that a high-salt diet could upregulate CYP2C11 and CYP2C23 in rat kidneys (Holla et al., 1999), and a further study confirmed that

TABLE 4

Plasma pharmacokinetic parameters after treatment with 10 mg/kg TOL in CYP2C11-null rats and WT rats

All values are shown as the mean ± S.D., n = 6. *P < 0.05; **P < 0.01 *compared with that of males in the same strain.*

Parameter	Male		Female	
	WT	Null	WT	Null
$AUC_{0\text{-}t}$ (μg/ml per hour)	648.62 ± 122.41	682.17 ± 97.42	1005.71 ± 54.53*	1037.04 ± 218.00*
$AUC_{0\text{-}\infty}$ (μg/ml per hour)[a]	675.66 ± 123.95	706.06 ± 93.97	1267.84 ± 99.70*	1170.57 ± 271.00*
C_{max} (μg/ml)[a]	49.67 ± 10.07	56.65 ± 10.98	68.97 ± 9.41*	82.85 ± 13.27*
T_{max} (h)[a]	4.08 ± 2.38	2.08 ± 1.50	1.75 ± 0.76	1.17 ± 0.41*
V_d/F (ml/kg)	143.42 ± 34.52	131.94 ± 15.10	182.51 ± 38.97	147.35 ± 21.68
Cl/F (ml/h per kilogram)	15.24 ± 2.93	14.38 ± 1.98	7.93 ± 0.68**	8.97 ± 2.25*

$AUC_{0\text{-}\infty}$, area under the curve; $AUC_{0\text{-}t}$, area under the blood concentration-time curve; CL/F, apparent oral clearance; C_{max}, peak concentration; T_{max}, time to reach C_{max}; V_d/F, Apparent Volume of Distribution.

decreased renal CYP2C11 and CYP2C23 levels were associated with angiotensin salt-sensitive hypertension (Holla et al., 1999; Zhao et al., 2003). Although CYP2C23 expressed higher levels in rat kidneys, the maximal reaction rate of CYP2C11 was considerably higher than that of CYP2C23 (5.1 ± 0.5 and 1.5 ± 0.1 nmol product/min/nmol P450 for CYP2C11 and CYP2C23, respectively) (Holla et al., 1999). Therefore, it remains unclear whether CYP2C11 or CYP2C23 played a more important role in epoxyeicosatrienoic acid–mediated blood pressure regulation. Our *CYP2C11*-null rat model would be an excellent tool to obtain conclusive results for this question.

In conclusion, a *CYP2C11*-null rat model was successfully generated and no off-target cleavage was detected at 11 predicted sites. Male *CYP2C11*-null rats seemed to have impaired fertility compared with WT males. CYP2B, CYP2D, and CYP4A1 expression was induced in the livers of male *CYP2C11*-null rats. TOL was used as a probe to study CYP2C11 enzyme activity. However, major differences were only observed in our in vitro investigations. Further studies with this model are needed to determine the in vivo function of CYP2C11.

Acknowledgments

We thank Miao Chen at the Department of Pathology, First People's Hospital, Zhenjiang, China, for performing histopathological analysis on the rat tissue samples.

Authorship Contributions

Participated in research design: Wei, Yang, Guo.
Conducted experiments: Yang, Zhang, Sui, C. Wang, K. Wang.
Performed data analysis: Wei, Shan.
Wrote or contributed to the writing of the manuscript: Wei, Yang, H. Wang.

References

Bae S, Park J, and Kim JS (2014) Cas-OFFinder: a fast and versatile algorithm that searches for potential off-target sites of Cas9 RNA-guided endonucleases. *Bioinformatics* **30**:1473–1475.
Banerjee S, Das RK, Giffear KA, and Shapiro BH (2015) Permanent uncoupling of male-specific CYP2C11 transcription/translation by perinatal glutamate. *Toxicol Appl Pharmacol* **284**:79–91.
Barbosa-Sicard E, Markovic M, Honeck H, Christ B, Muller DN, and Schunck WH (2005) Eicosapentaenoic acid metabolism by cytochrome P450 enzymes of the CYP2C subfamily. *Biochem Biophys Res Commun* **329**:1275–1281.
Brown HS, Chadwick A, and Houston JB (2007) Use of isolated hepatocyte preparations for cytochrome P450 inhibition studies: comparison with microsomes for K_i determination. *Drug Metab Dispos* **35**:2119–2126.
Capdevila JH, Falck JR, and Imig JD (2007) Roles of the cytochrome P450 arachidonic acid monooxygenases in the control of systemic blood pressure and experimental hypertension. *Kidney Int* **72**:683–689.
Choi HK and Waxman DJ (2000) Plasma growth hormone pulse activation of hepatic JAK-STAT5 signaling: developmental regulation and role in male-specific liver gene expression. *Endocrinology* **141**:3245–3255.
Cong L, Ran FA, Cox D, Lin S, Barretto R, Habib N, Hsu PD, Wu X, Jiang W, Marraffini LA, et al. (2013) Multiplex genome engineering using CRISPR/Cas systems. *Science* **339**:819–823.
Cradick TJ, Qiu P, Lee CM, Fine EJ, and Bao G (2014) COSMID: a web-based tool for identifying and validating CRISPR/Cas off-target sites. *Mol Ther Nucleic Acids* **3**:e214.
Cribb AE, Spielberg SP, and Griffin GP (1995) N4-hydroxylation of sulfamethoxazole by cytochrome P450 of the cytochrome P4502C subfamily and reduction of sulfamethoxazole hydroxylamine in human and rat hepatic microsomes. *Drug Metab Dispos* **23**:406–414.
Daskalopoulos EP, Malliou F, Rentesi G, Marselos M, Lang MA, and Konstandi M (2012) Stress is a critical player in *CYP3A*, *CYP2C*, and *CYP2D* regulation: role of adrenergic receptor signaling pathways. *Am J Physiol Endocrinol Metab* **303**:E40–E54.
Ding XX and Coon MJ (1990) Immunochemical characterization of multiple forms of cytochrome P-450 in rabbit nasal microsomes and evidence for tissue-specific expression of P-450s NMa and NMb. *Mol Pharmacol* **37**:489–496.
Dostalek M, Jurica J, Pistovcakova J, Hanesova M, Tomandl J, Linhart I, and Sulcova A (2007) Effect of methamphetamine on cytochrome P450 activity. *Xenobiotica* **37**:1355–1366.
Gonzalez FJ and Kimura S (2003) Study of P450 function using gene knockout and transgenic mice. *Arch Biochem Biophys* **409**:153–158.
Gonzalez FJ and Yu AM (2006) Cytochrome P450 and xenobiotic receptor humanized mice. *Annu Rev Pharmacol Toxicol* **46**:41–64.
Gu J, Weng Y, Zhang QY, Cui H, Behr M, Wu L, Yang W, Zhang L, and Ding X (2003) Liver-specific deletion of the NADPH-cytochrome P450 reductase gene: impact on plasma cholesterol homeostasis and the function and regulation of microsomal cytochrome P450 and heme oxygenase. *J Biol Chem* **278**:25895–25901.
Heigwer F, Kerr G, and Boutros M (2014) E-CRISP: fast CRISPR target site identification. *Nat Methods* **11**:122–123.
Heil SG, De Vriese AS, Kluijtmans LA, Dijkman H, van Strien D, Akkers R, and Blom HJ (2005) Cytochrome P450-2C11 mRNA is not expressed in endothelial cells dissected from rat renal arterioles. *Nephron, Physiol* **99**:p43–p49.
Holla VR, Makita K, Zaphiropoulos PG, and Capdevila JH (1999) The kidney cytochrome P-450 2C23 arachidonic acid epoxygenase is upregulated during dietary salt loading. *J Clin Invest* **104**:751–760.
Honkakoski P and Negishi M (2000) Regulation of cytochrome P450 (CYP) genes by nuclear receptors. *Biochem.J* **347**:321–337.
Imig JD (2010) Targeting epoxides for organ damage in hypertension. *J Cardiovasc Pharmacol* **56**:329–335.
Johnson EF, Palmer CN, Griffin KJ, and Hsu MH (1996) Role of the peroxisome proliferator-activated receptor in cytochrome P450 4A gene regulation. *FASEB J* **10**:1241–1248.
Kőhalmy K, Tamási V, Kóbori L, Sárváry E, Pascussi JM, Porrogi P, Rozman D, Prough RA, Meyer UA, and Monostory K (2007) Dehydroepiandrosterone induces human CYP2B6 through the constitutive androstane receptor. *Drug Metab Dispos* **35**:1495–1501.
Lin Y, Cradick TJ, Brown MT, Deshmukh H, Ranjan P, Sarode N, Wile BM, Vertino PM, Stewart FJ, and Bao G (2014) CRISPR/Cas9 systems have off-target activity with insertions or deletions between target DNA and guide RNA sequences. *Nucleic Acids Res* **42**:7473–7485.
Ma Y, Zhang X, Shen B, Lu Y, Chen W, Ma J, Bai L, Huang X, and Zhang L (2014) Generating rats with conditional alleles using CRISPR/Cas9. *Cell Res* **24**:122–125.
Martignoni M, Groothuis GM, and de Kanter R (2006) Species differences between mouse, rat, dog, monkey and human CYP-mediated drug metabolism, inhibition and induction. *Expert Opin Drug Metab Toxicol* **2**:875–894.
Matsunaga N, Nishijima T, Hattori K, Iizasa H, Yamamoto K, Kizu J, Takanaka A, Morikawa A, and Nakashima E (2001) Application of the PKCYP-test to predict the amount of in vivo CYP2C11 using tolbutamide as a probe. *Biol Pharm Bull* **24**:1305–1310.
McKinnon RA and Nebert DW (1998) Cytochrome P450 knockout mice: new toxicological models. *Clin Exp Pharmacol Physiol* **25**:783–787.
Morgan ET, MacGeoch C, and Gustafsson JA (1985) Hormonal and developmental regulation of expression of the hepatic microsomal steroid 16α-hydroxylase cytochrome P-450 apoprotein in the rat. *J Biol Chem* **260**:11895–11898.
Muruganandan S and Sinal CJ (2008) Mice as clinically relevant models for the study of cytochrome P450-dependent metabolism. *Clin Pharmacol Ther* **83**:818–828.
Nedelcheva V and Gut I (1994) P450 in the rat and man: methods of investigation, substrate specificities and relevance to cancer. *Xenobiotica* **24**:1151–1175.
Rahmaniyan M, Patrick K, and Bell NH (2005) Characterization of recombinant CYP2C11: a vitamin D 25-hydroxylase and 24-hydroxylase. *Am J Physiol Endocrinol Metab* **288**:E753–E760.
Rendic S and Di Carlo FJ (1997) Human cytochrome P450 enzymes: a status report summarizing their reactions, substrates, inducers, and inhibitors. *Drug Metab Rev* **29**:413–580.
Ripp SL, Falkner KC, Pendleton ML, Tamasi V, and Prough RA (2003) Regulation of CYP2C11 by dehydroepiandrosterone and peroxisome proliferators: identification of the negative regulatory region of the gene. *Mol Pharmacol* **64**:113–122.
Roman RJ (2002) P-450 metabolites of arachidonic acid in the control of cardiovascular function. *Physiol Rev* **82**:131–185.
Ryan DE and Levin W (1990) Purification and characterization of hepatic microsomal cytochrome P-450. *Pharmacol Ther* **45**:153–239.
Schaefer KA, Wu WH, Colgan DF, Tsang SH, Bassuk AG, and Mahajan VB (2017) Unexpected mutations after CRISPR-Cas9 editing in vivo. *Nat Methods* **14**:547–548.
Tan Z, Ma Y, Shi R, and Chen Y (2011) Effect of *Scutellaria baicalensis* on the pharmacokinetics of tolbutamide in rats. *Chin Tradit Pat Med* **7**:1153–1158.
Timsit YE and Negishi M (2014) Coordinated regulation of nuclear receptor CAR by CCRP/DNAJC7, HSP70 and the ubiquitin-proteasome system. *PLoS One* **9**:e96092.
Velenosi TJ, Fu AY, Luo S, Wang H, and Urquhart BL (2012) Down-regulation of hepatic CYP3A and CYP2C mediated metabolism in rats with moderate chronic kidney disease. *Drug Metab Dispos* **40**:1508–1514.
Veronese ME, McManus ME, Laupattarakasem P, Miners JO, and Birkett DJ (1990) Tolbutamide hydroxylation by human, rabbit and rat liver microsomes and by purified forms of cytochrome P-450. *Drug Metab Dispos* **18**:356–361.
Wang H, Cheng JD, Montgomery D, and Cheng KC (2009) Evaluation of the binding orientations of testosterone in the active site of homology models for CYP2C11 and CYP2C13. *Biochem Pharmacol* **78**:406–413.
Wang X, Lee WY, Or PM, and Yeung JH (2010) Pharmacokinetic interaction studies of tanshinones with tolbutamide, a model CYP2C11 probe substrate, using liver microsomes, primary hepatocytes and in vivo in the rat. *Phytomedicine* **17**:203–211.
Wang X, Tang Y, Lu J, Shao Y, Qin X, Li Y, Wang L, Li D, and Liu M (2016) Characterization of novel cytochrome P450 2E1 knockout rat model generated by CRISPR/Cas9. *Biochem Pharmacol* **105**:80–90.
Waxman DJ (1988) Interactions of hepatic cytochromes P-450 with steroid hormones. Regioselectivity and stereospecificity of steroid metabolism and hormonal regulation of rat P-450 enzyme expression. *Biochem Pharmacol* **37**:71–84.
Webb SJ, Geoghegan TE, Prough RA, and Michael Miller KK (2006) The biological actions of dehydroepiandrosterone involves multiple receptors. *Drug Metab Rev* **38**:89–116.
Wójcikowski J and Daniel WA (2009) The brain dopaminergic system as an important center regulating liver cytochrome P450 in the rat. *Expert Opin Drug Metab Toxicol* **5**:631–645.
Wójcikowski J, Haduch A, and Daniel WA (2013) Effect of antidepressant drugs on cytochrome P450 2C11 (CYP2C11) in rat liver. *Pharmacol Rep* **65**:1247–1255.
Wu HQ, Masset-Brown J, Tweedie DJ, Milewich L, Frenkel RA, Martin-Wixtrom C, Estabrook RW, and Prough RA (1989) Induction of microsomal NADPH-cytochrome P-450 reductase and cytochrome P-450IVA1 ($P\text{-}450_{LA\omega}$) by dehydroepiandrosterone in rats: a possible peroxisomal proliferator. *Cancer Res* **49**:2337–2343.
Zhao X, Pollock DM, Inscho EW, Zeldin DC, and Imig JD (2003) Decreased renal cytochrome P450 2C enzymes and impaired vasodilation are associated with angiotensin salt-sensitive hypertension. *Hypertension* **41**:709–714.

Address correspondence to: Dr. Yuan Wei, School of Pharmacy, Jiangsu University, No. 301, Xuefu Road, Jingkou District, Zhenjiang, Jiangsu 212013, China. E-mail: ywei@ujs.edu.cn

Drug Metabolism and Disposition

Generation and Characterization of a CYP2C11-null Rat Model by using the CRISPR/Cas9 method

Y Wei, L Yang, X Zhang, D Sui, C Wang, K Wang, M Shan, D Guo, H Wang

	20	19	18	17	16	15	14	13	12	11	10	9	8	7	6	5	4	3	2	1
gRNA	T	C	A	A	G	G	G	T	A	A	A	C	T	C	A	G	A	C	T	G
R-01	G							G												
R-02		G										G								
R-03							T	A												
R-04								A					G							
R-05								A									C			
R-06								C							T					
R-07								C										G		
R-08									T		G									
R-09									T								C			
R-10											C							G		
R-11														T			T			

Supplemental Figure 1. Eleven potential off-target sites for sgRNA, marked in red and shaded. The shaded boxes show mismatches between the gRNA sequence and the listed off-target sites.

Drug Metabolism and Disposition

Generation and Characterization of a CYP2C11-null Rat Model by using the CRISPR/Cas9 method

Y Wei, L Yang, X Zhang, D Sui, C Wang, K Wang, M Shan, D Guo, H Wang

Supplemental Table 1. Primers used to amplify DNA sequences containing potential off-target sites

	Forward primer (5'-3')	Reverse primer (5'-3')
R-01	GTTTGCTTTCGTGGGTGTG	GGTTCAGTCTCCTCAGTAAGAG
R-02	GGAAGAGGTAGGATGAACAGACT	GAGAAGGAAGAAAGGAAAGG
R-03	TGACTTAGCCGTGAGCAGTT	ACAAGTGGAACGAAAGGAGAAG
R-04	CTTTGTTCTCTAACTGCTTGCT	TCTTGTCTACTAGGTGCTCTTG
R-05	ATGGTGAGACAAGGTGTGGTAA	ACAGTCTATAATAAGTATGCGGAGC
R-06	CCAGAAGCCAGAATAACAAGAT	CGATATTAGAGTGCCAGTGTG
R-07	CTTGTGCCTAGCGTGAGTCTG	CCTCTTGCATCCTGCTTGTCTT
R-08	AGAAGGAGGCAAGGTCACA	GGTGTTCAAACCAAGCCATAT
R-09	TGAGTTACACGGTGAGAATCCA	AGCATCACACGGCAAGAGAA
R-010	GAGCAGACATATGGACAGGAG	AATAGCAGAAGAACTTGGTGGT
R-011	CACTGGTGATGCTTAATGAGG	CACTGCTTGTCTGGATTGC